

## Application of ZnO and TiO<sub>2</sub> nanoparticles coated onto montmorillonite in the presence of H<sub>2</sub>O<sub>2</sub> for efficient removal of cephalexin from aqueous solutions

Rasoul Khosravi\*, Ahmad Zarei\*\*, Mohsen Heidari\*\*\*, Ali Ahmadfazeli\*\*\*\*, Mehdi Vosughi\*\*\*\*, and Mehdi Fazlzadeh\*\*\*\*\*,†

\*Social Determinants of Health Research Center, Department of Environmental Health Engineering, School of Health, Birjand University of Medical Sciences, Birjand, Iran

\*\*Environmental Health Engineering, Department of Environmental Health Engineering, School of Public Health, Gonabad University of Medical Sciences, Gonabad, Iran

\*\*\*Department of Environmental Health Engineering, Faculty of Health, Hormozgan University of Medical Sciences, Bandar Abbas, Iran

\*\*\*\*Department of Environmental Health Engineering, School of Public Health, Ardabil University of Medical Sciences, Ardabil, Iran

\*\*\*\*\*Social Determinants of Health Research Center, Department of Environmental Health Engineering, School of Public Health, Ardabil University of Medical Sciences, Ardabil, Iran

(Received 25 June 2017 • accepted 11 January 2018)

**Abstract**—This study considers the feasibility of uptake of cephalexin, an emerging contaminant, from aqueous solutions by using green local montmorillonite (GLM), montmorillonite coated with ZnO (ZnO/GLM) and montmorillonite coated with TiO<sub>2</sub> (TiO<sub>2</sub>/GLM) in the presence of H<sub>2</sub>O<sub>2</sub>. Batch adsorption experiments were carried out as a function of pH, initial concentration of the cephalexin, adsorbent dosage, contact time, and temperature. Finally, the adsorbents were characterized by XRD, SEM and FTIR analyses. XRD patterns showed dramatic changes in the adsorbents after loading with the nanoparticles, confirming successful placing of the nanoparticles onto GLM. The GLM mineral surface after nanoparticle loading appears to be fully exposed and more porous with irregular shapes in particles diameters of 1-50 microns. FTIR analyses also confirmed dramatic changes in surface functional groups after modification with these nanoparticles. The results showed that the removal efficiency of cephalexin was better at lower pH values. Totally, the removal efficiency increased with increase in adsorbent dosage and contact time and decreased with concentration and temperature increase. The thermodynamics values of  $\Delta G^\circ$  and  $\Delta H^\circ$  revealed that the adsorption process was spontaneous and exothermic. In isotherm study, the maximum adsorption capacities (qm) were obtained to be 7.82, 17.09 and 49.26 mg/g for GLM, ZnO/GLM and TiO<sub>2</sub>/GLM, respectively. Temkin constant ( $B_T$ ) showed that adsorption of cephalexin from solution was exothermic for all three adsorbents.

Keywords: Adsorption, Cephalexin, Montmorillonite, Nanoparticles

### INTRODUCTION

Antibiotic agents have been applied in large quantities for the control of human and veterinary microbial infections and also for aquaculture applications [1,2]. However, about 30 to 90% of the antibiotics is not completely metabolized in the human body and is excreted through urine and feces, with eventual discharge into the surrounding environment as harmful compounds [3]. Such extensive use results in the release of large amounts of antibiotics in industrial effluents and aquatic environment which need to be properly treated before discharging into the streams and water bodies [4]. Unfortunately, conventional treatment procedures cannot efficiently remove antibiotics in sewage treatment plants [5]. Although their levels in the receiving waters are low, their continual introduction

into the environment for a long period can cause health problems in the near future, including the promotion and development and spread of antibiotic resistance species, change in microbial ecology and transfer into food chain and subsequently, unexpected effects on human health [6]. Cephalexin is a kind of semisynthetic cephalosporin antibiotic that is extensively used for the treatment of infections in humans or animals [7,8]. Accumulated levels of cephalexin in drinking water can result in mutagenic and carcinogenic effects in the human body [8]. Various procedures, such as bioaugmentation, solid phase extraction, liquid membrane separation, nanofiltration, electro-Fenton oxidation, enzymatic complexation and sono-chemical degradation, have been utilized for uptake of cephalexin from aqueous environments [9]. Adsorption is an effective separation process to remove contaminants within water and wastewater that has advantages in terms of ease of operation, cost, flexibility and simplicity of design compared to other methods [10-12]. Among adsorbents, clay minerals are inexpensive adsorbents and are extensively used in various water treatment processes due

†To whom correspondence should be addressed.

E-mail: m.fazlzadeh@gmail.com

Copyright by The Korean Institute of Chemical Engineers.

to their eco-friendliness, easy availability, non-toxicity, presence of several types of active binding sites on the surface and large surface area [13,14]. Raw and modified clays have been utilized as efficient adsorbents for the removal of various dyes, pesticides and antibiotics [15,16]. In large scale applications, these minerals can be alternative adsorbents to activated carbons [9]. Many studies have been focused on coating nanoparticles onto clay minerals in order to considerably improve the adsorption efficiencies of the materials for the adsorption of different contaminants from aqueous solutions. Recently, considerable attention has been centered upon the use of nanomaterials due to their special properties [17, 18]. Nanoparticles range in size from 1 to 100 nm [19]. Most of the atoms are available on the surface which can easily bind with the other atoms to remove contaminants from aqueous environment. In addition, due to high surface to volume ratio of nano-materials, their adsorption capacity could be greatly increased [17,20, 21]. Literature studies about the surface of various oxidants including  $\text{TiO}_2$ ,  $\text{Al}_2\text{O}_3$ ,  $\text{ZrO}_2$ ,  $\text{CeO}_2$  and  $\text{ZnO}$  showed that the materials had relatively high adsorption capacities. The adsorption properties of the oxides, including  $\text{TiO}_2$  nanoparticles, strongly depend on the characteristics of the solid, e.g., morphology, crystal structure, specific surface area, defects, surface impurities, hydroxyl coverage and modifiers [22]. Control of these items can be achieved by applying an appropriate synthetic or modified procedure. However, some previous studies in the literature applied strong oxidants such as  $\text{HNO}_3$ ,  $\text{KMnO}_4$ ,  $\text{O}_3$  and  $\text{H}_2\text{O}_2$  in surface modifications to increase the adsorption capacities of different adsorbents [23]. In the present study, we used a green local montmorillonite collected from Sarcheshmeh region in Ardabil, Iran as a support material for  $\text{TiO}_2$  and  $\text{ZnO}$  nanoparticles.  $\text{H}_2\text{O}_2$  was applied for the stabilization of  $\text{TiO}_2$  and  $\text{ZnO}$  nanoparticles onto montmorillonite. Then, the adsorption efficiency of the new sorbents was evaluated for the removal of cephalexin.

## MATERIALS AND METHODS

### 1. Materials

This research was carried out experimentally on a batch basis. All of the chemicals were obtained from Sigma-Aldrich Company. Commercial  $\text{TiO}_2$  and  $\text{ZnO}$  nanoparticles used for the adsorbent preparation were obtained from Mehregan Shimi Company. The size of the  $\text{TiO}_2$  and  $\text{ZnO}$  nanoparticles was less than 20 nm.

### 2. Preparation of the Adsorbents

Green local montmorillonite (GLM) clay was collected from Sarcheshmeh region in Ardabil, Iran. After crushing in a laboratory mill, it was sieved and other impurities were removed. After that, it was sun dried for two days. The clay was washed several times with distilled water to remove any color and remaining impurities and oven dried for 24 h at 60 °C. Again, it was sieved through a 10 mesh screen to obtain uniform and smaller particle sizes and stored in a desiccator for further use.

### 3. Modification Process

For loading  $\text{TiO}_2$  and  $\text{ZnO}$  nanoparticles onto prepared montmorillonite, 200 mL of double distilled water was poured into a beaker having 1 g of each nanoparticle and agitated at 300 rpm. Thereafter, 100 g of montmorillonite was added to the solution and

mixed for 1 h to be uniformly distributed. At this stage, potassium permanganate and hydrogen peroxide were added into the solution drop by drop to stabilize the nanoparticles onto the clay. Then, the prepared montmorillonite was dried in an oven for 24 h at 100 °C. The resulting sample was transferred to a furnace at 500 °C for 2 h for stabilization. Finally, the resulting adsorbent was kept in a container in absence of moisture to be used for conducting the adsorption experiments. The value of  $\text{pH}_{\text{Pzc}}$  of the adsorbent was determined. Finally, the materials were characterized by SEM images and FTIR spectrum to determine surface and functional properties of the prepared adsorbents.

### 4. Adsorption Experiments

Batch experiments were carried out for cephalexin adsorption using a 100 mL Erlenmeyer flask on the shaker. Cephalexin powder obtained from Iran Daru Company was used for preparation of required concentrations of cephalexin. For the experiments, initially 50 mL of the sample with desired concentration was added into each Erlenmeyer flask, and the pH of the solution was adjusted to the desired values by adding HCl and NaOH. Then a predetermined mass of the adsorbent was added into each Erlenmeyer flask and immediately placed on a shaker. The samples were collected and analyzed for determination of residual concentration of cephalexin at regular time intervals during the adsorption process. We aimed at providing insight into the influence of main operating parameters, such as initial pH (2-11), adsorbent dosage (1-10 g), contact time (1-150 min), cephalexin concentration (25-200 mg/L), temperature (10-40 °C), agitation speed (0-200 rpm) on the adsorption of cephalexin. All the experiments were conducted in duplicate and the mean values were reported.

### 5. Determination of Cephalexin Concentration

Residual concentration of cephalexin was determined from the absorbance of the solution measured by a spectrophotometer (model Lambda 25, PerkinElmer) at a wavelength of 216 nm according to Standard Methods for the Examination of Water and Wastewater. Adsorbents characteristics including surface area, crystalline structure and functional groups were determined by use of XRD, FTIR and SEM analyses.

## RESULTS AND DISCUSSION

### 1. Adsorbent Characterization

XRD is one of the preferred procedures to follow the structural

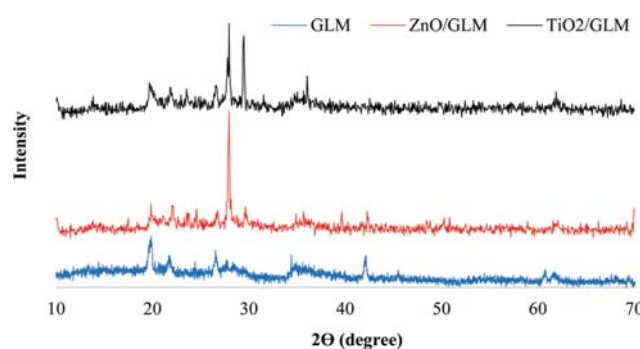


Fig. 1. XRD patterns of GLM, ZnO/GLM, and  $\text{TiO}_2$ /GLM.

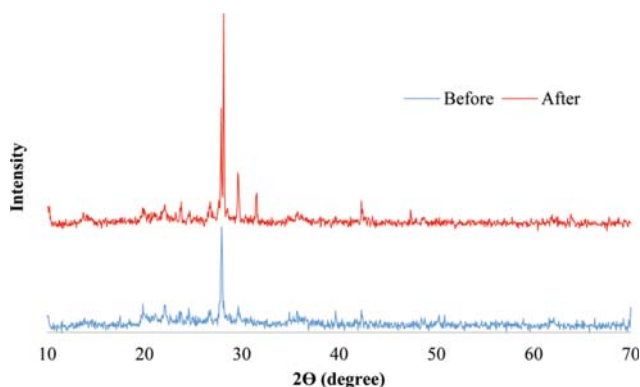


Fig. 2. XRD patterns of ZnO/GLM before and after adsorption of cephalexin.

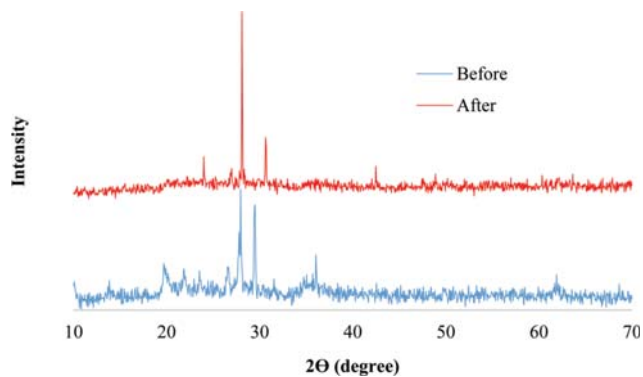


Fig. 3. XRD patterns of TiO<sub>2</sub>/GLM before and after adsorption of cephalexin.

changes caused after modification of an adsorbent. XRD patterns of green montmorillonite (GLM), GLM coated with ZnO and GLM coated with TiO<sub>2</sub> are depicted in Fig. 3. As can be seen, after nanoparticles loading in the presence of H<sub>2</sub>O<sub>2</sub>, strong peaks of  $2\theta=28.8$  and  $2\theta=27.95$  belonging to SiO<sub>2</sub> become stronger compared to the other peaks [24]. The change in the phases can be attributed to the oxidant activity of H<sub>2</sub>O<sub>2</sub> in oxidation of some metals in the

GLM structure. As the amount of nanoparticle loading onto GLM is 1% W/W, the XRD analysis cannot detect the small amounts of nanoparticles on GLM [25]. However, Xue et al. reported that modification of an adsorbent by H<sub>2</sub>O<sub>2</sub> has little influence on the mineral components of adsorbent [26].

Fig. 4 shows scanning electron microscopy (SEM) micrographs of the adsorbents. Fig. 4(a), (b) show GLM surface before the nano-

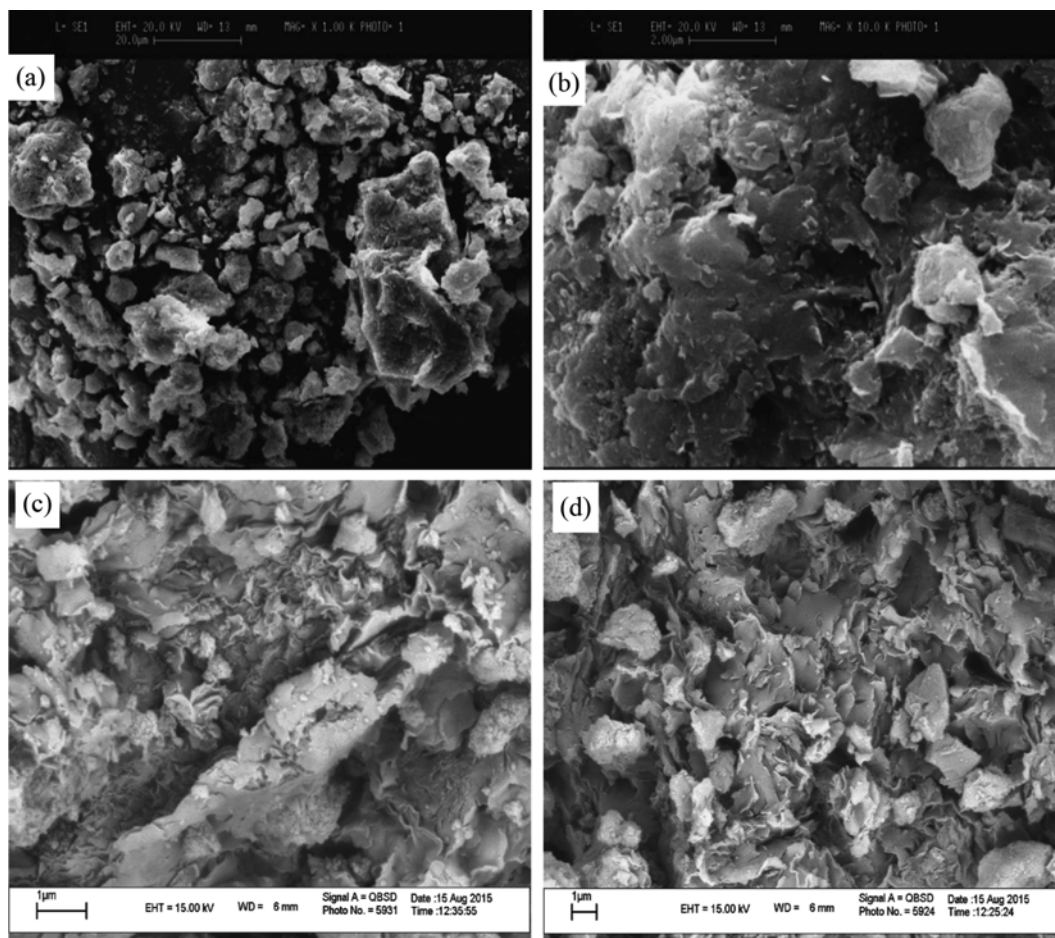


Fig. 4. SEM images of GLM (a) and (b), ZnO/GLM (c), and TiO<sub>2</sub>/GLM (d).

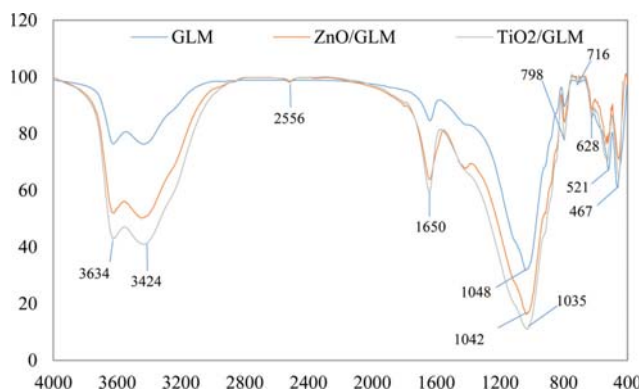


Fig. 5. FTIR spectra GLM, ZnO/GLM and TiO<sub>2</sub>/GLM.

particles loading, respectively in two magnifications. As observed from the figure, GLM particles are rough and feature a high porous structure, with irregular shapes in range of 1-50 microns. Also, in Fig. 4(b), the surface of the GLM is covered with a small number of pores and is rough and homogeneous. Fig. 4(c) and 4(d) also show ZnO/GLM and TiO<sub>2</sub>/GLM, respectively. After treatment with H<sub>2</sub>O<sub>2</sub>, the surface of the adsorbents becomes layered and rough. Also, the adsorbent surfaces changed dramatically with many pores on the surfaces after ZnO and TiO<sub>2</sub> loading. These changes on the surface were likely to result in highly porous structure, resulting in a high surface area for better adsorption of cephalaxin. Small particles in the SEM image confirm the loaded nanoparticles on GLM. However, Xue et al. reported that use of H<sub>2</sub>O<sub>2</sub> has a little influence but not enough to increase the number of pores or change the adsorbent structure that could dramatically increase the adsorbent surface [26].

## 2. FTIR Spectroscopy

The functional groups of the adsorbents were detected using Fourier transform infrared spectroscopy (FTIR) in a range of 400 to 4,000 cm<sup>-1</sup>. The FTIR spectra of GLM, ZnO/GLM and TiO<sub>2</sub>/GLM are shown in Fig. 5. The results revealed the presence of different functional groups on the surface of these adsorbents. The bands detected in 3,224 and 3,634 cm<sup>-1</sup> regions were attributed to O-H stretching vibrations [27]. Also, the bands at 1,053 cm<sup>-1</sup> were attributed to Si-O-Si stretching vibrations. The bands in range of 1,650-1,636 cm<sup>-1</sup> were assigned to the bending vibrations of hydroxyl functional groups [28]. The peaks of 521 and 467 cm<sup>-1</sup> in GLM modified with TiO<sub>2</sub> belong to Al-O-Si and Si-O-Fe. Coating GLM with TiO<sub>2</sub> nanoparticles displace above peaks to 530 and 462 cm<sup>-1</sup>. For ZnO/GLM, the peaks changed to 538 and 470 cm<sup>-1</sup>. Furthermore, considerable changes of the peaks at 3,638-3,420 cm<sup>-1</sup> and 1,630-1,650 cm<sup>-1</sup> for GLM coated with TiO<sub>2</sub> nanoparticles and GLM coated with ZnO nanoparticles revealed the increase of some functional groups such as hydroxyl. This increase in the number of oxygenated groups is due to the application of H<sub>2</sub>O<sub>2</sub> in the process of nanoparticles loading [26].

## 3. Effect of Contact Time

Contact time between adsorbate and adsorbent is an important parameter in adsorption process. The effect of contact time on the adsorption of cephalaxin onto GLM, ZnO/GLM and TiO<sub>2</sub>/GLM was examined (see Fig. 6). The adsorption rates of cephalaxin by

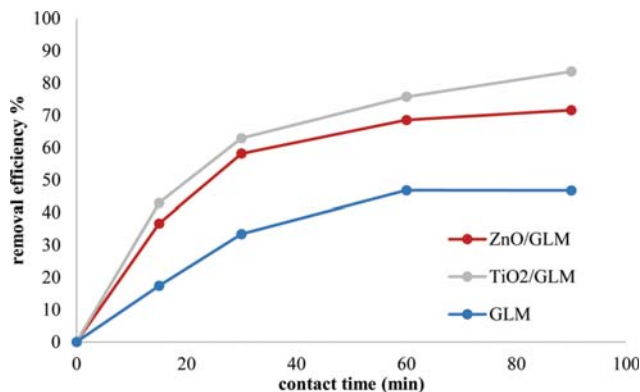


Fig. 6. Effect of contact time on the adsorption of cephalaxin by GLM, ZnO/GLM and TiO<sub>2</sub>/GLM (pH=7, cephalaxin concentration=25 mg/l, agitation speed=150 rpm and dosage=4 g/L).

the three adsorbents were fast within the first 30 min of the adsorption process because of the presence of numerous vacant adsorption sites at the early stages of the process. Beyond 30 min, removal percentages reduced gradually. Generally, an adsorbent is ideal when it adsorbs a contaminant in low contact time with a high removal yield. From Fig. 6, cephalaxin adsorption was rapid for the first 30 min, and later it decreased gradually and finally attained equilibrium after 60 min, which the amount of the contaminant adsorbed was negligible. Therefore, we considered 60 min as an optimum contact time for the antibiotic adsorption. Generally, adsorption of cephalaxin occurred in two stages. At first 30 min, the adsorption was rapid, which was due to external surface adsorption. After 30 min, the uptake increased at a lower rate, which can be attributed to internal surface adsorption [29]. Fig. 6 also illustrates that GLM coated with the nanoparticles can adsorb cephalaxin in lower contact time that GLM alone. Accordingly, adsorption percentage of the antibiotic by TiO<sub>2</sub>/GLM at 60 min was about 30% more than that of GLM.

## 4. Effect of Agitation Speed

Fig. 7 depicts the influence of agitation speed on the removal efficiency of cephalaxin by GLM, ZnO/GLM and TiO<sub>2</sub>/GLM. The

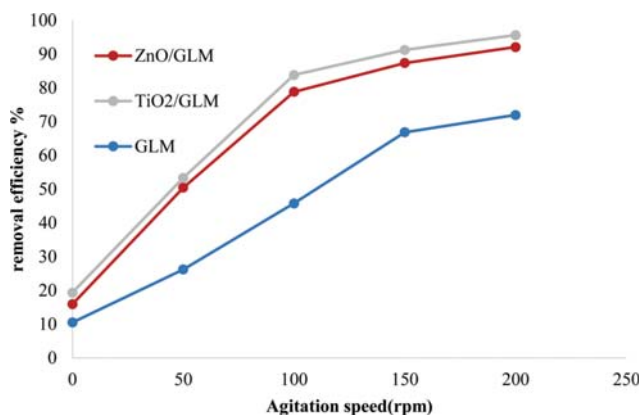


Fig. 7. Effect of agitation speed on the adsorption of cephalaxin by GLM, ZnO/GLM and TiO<sub>2</sub>/GLM (pH=2, cephalaxin concentration=25 mg/l, contact time=60 min, dosage=4 g/L).

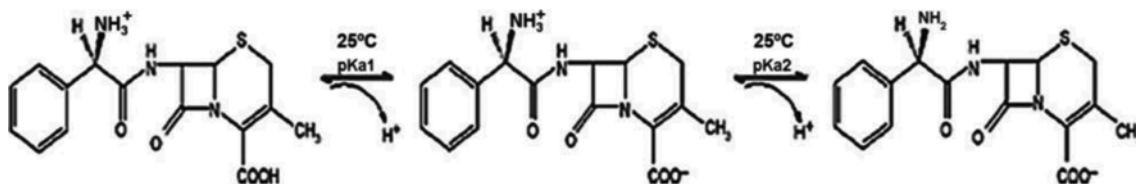


Fig. 8. Cephalosporin ionization states:  $pK_{a1}=2.56$ ,  $pK_{a2}=6.88$ , isoelectric point=4.5.

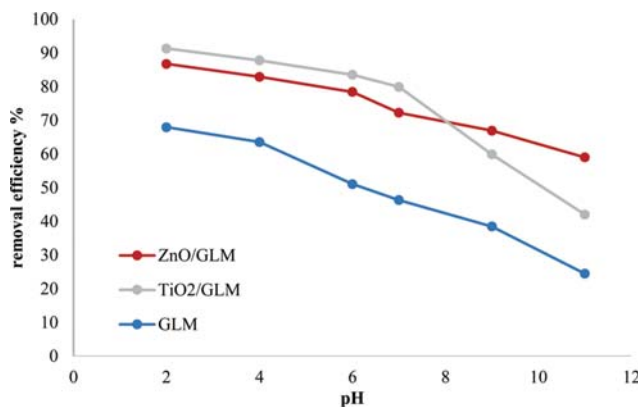


Fig. 9. Effect of pH on the adsorption of cephalosporin by GLM, ZnO/GLM and TiO<sub>2</sub>/GLM (cephalosporin concentration=25 mg/l, contact time=60 min, and dosage=4 g/L, agitation speed=150 rpm).

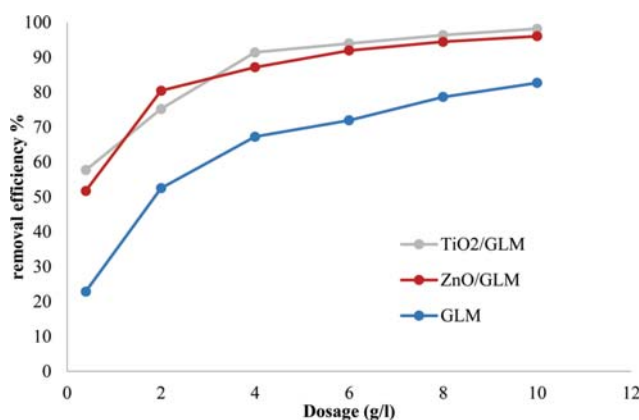


Fig. 10. Effect of adsorbent dosage on the adsorption of cephalosporin by GLM, ZnO/GLM and TiO<sub>2</sub>/GLM (pH=2, contact time=60 min, dosage=4 g/L, agitation speed=150 rpm).

overall adsorption efficiency increased significantly with an increase in the agitation speed. The removal efficiencies of cephalosporin by GLM and TiO<sub>2</sub>/GLM were 10.52 and 19.23%, respectively, in the absence of agitation. In the case of agitation at 200 rpm, the removal efficiencies increased to 95.6 and 71.96%, respectively. By increasing the agitation speed, the interactions between adsorbate and adsorbent become higher due to enhanced turbulence as the thickness of the liquid boundary layer decreases, which in general increase the removal efficiency of contaminants in the solution [30].

### 5. Effect of Solution pH

Solution pH is an intrinsic item that influences the adsorption process by affecting the solution chemistry of contaminants and the activity of functional groups of the adsorbent surface. Fig. 9 shows the effect of solution pH on the removal of cephalosporin by GLM, ZnO/GLM and TiO<sub>2</sub>/GLM at contact time of 60 min. The highest removal efficiency was observed at pH=2. Therefore, pH=2 was considered for optimization and the experiments. Note that the removal efficiency decreased with increase in pH value. For example, at pH=2 the removal percentage of cephalosporin by TiO<sub>2</sub>/GLM was 91.23%, which decreased to 42.04% at pH=11. This can be attributed to the cationic structure of cephalosporin at pH<2.56 and pH<sub>pzc</sub> (pH point of zero charge, pH at which charge transition of surface occurs) of the adsorbent which was at pH=8. Cephalosporin is a dipole ion with carboxyl and amino groups in its structure (Fig. 8). It is known that cephalosporin ion exists as a zwitterion, cationic and anionic chemical species depending on pH values [31].

Based on the pH<sub>pzc</sub>, it is expected that the adsorbent surface becomes negatively and positively charged at basic (pH>8) and acidic environments, respectively. A high removal efficiency of the anti-

biotic at acidic conditions indicates that the contaminant adsorbs on the adsorbents via its carboxyl groups [32]. At basic conditions, the levels of electrostatic repulsion forces between the antibiotic and negative sites on the surfaces of the adsorbents diminish, which reduces the removal efficiency of the contaminant from solution. Increase in the solution pH value increases the numbers of OH groups, which in general results in the decline in the positively charged binding sites, and therefore, the removal efficiency of cephalosporin decreases [33].

### 6. Effect of Adsorbent Dosage

The amount of adsorbent dosage used for this work is an important factor as it determines the removal percentages, as shown in Fig. 10. Specifically, the cephalosporin removal percentage increased from 33.72 to 44.36% with increasing GLM and TiO<sub>2</sub>/GLM dosages from 0.4 to 4 g/L, respectively. The present work shows that the removal percentage of cephalosporin increased with the increase in adsorbent dosage. This can be attributed to higher adsorbent surface area and availability of more binding sites resulting from the increasing amounts of adsorbent dosages [34]. As shown in Fig. 6, 0.4 g of GLM adsorbed 67% of cephalosporin. But at the same amount of TiO<sub>2</sub>/GLM and ZnO/GLM adsorbents, the removal efficiencies increased to 91.4 and 87.16%, respectively. The results of the present study agree with the results obtained by Noorimotlagh et al. who investigated wastewater sludge modified with zinc oxide for the adsorption of methylene blue from aqueous solutions. They reported removal capacities of 6.6 mg/g and 2.9 mg/g for nanoparticles and raw sludge, respectively. They found that removal efficiency of the adsorbent increased with loading zinc oxide nanoparticles onto wastewater sludge [35].

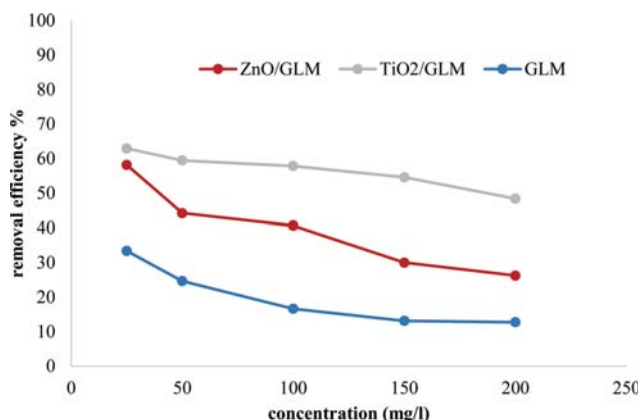


Fig. 11. Effect of initial concentration on cephalexin adsorption by GLM, TiO<sub>2</sub>/GLM and ZnO/GLM (pH=7, dosage=4 g/L, agitation speed=150 rpm).

### 7. Effect of Cephalexin Concentration

The initial concentration of a contaminant is another important factor, which influences the extent of contaminant uptake from the solution. Removal efficiency of cephalexin decreased with increase of initial concentration. Accordingly, as the initial concentration of cephalexin increased from 25 mg/L to 200 mg/L, the removal percentage of cephalexin onto TiO<sub>2</sub>/GLM and GLM decreased from 62.92 to 48.36% and 33.4 to 12.73%, respectively (Fig. 11). This indicates that the initial concentration strongly affects the removal efficiency. Moreover, this can be explained by the fact that more available binding sites were being covered as cephalexin concentration increased. However, the adsorption capacity at equilibrium increased with an increase in initial concentration of cephalexin. This can be attributed to an increasing concentration gradient of the contaminants, which acts as a driving force to overcome the resistance between the aqueous phase and the adsorbents [33]. Moussavi et al. studied the removal of amoxicillin antibiotic by NH<sub>4</sub>Cl-induced activated carbon. They found that by increasing the concentration of amoxicillin from 100 mg/L to 500 mg/L, the removal percentages of the antibiotic onto SAC and NAC decreased from 100 to 41.7% and from 99.3 to 68.3%, respectively, due to saturation of available binding sites on the adsorbent surface with concentration increase [36].

### 8. Effect of Temperature

Temperature is one of the key factors to consider in the adsorption process. Thus, the influence of temperature on cephalexin adsorption by GLM, ZnO/GLM and TiO<sub>2</sub>/GLM was examined and the findings are presented in Fig. 12. When the solution temperature was increased from 10 to 50 °C, the removal efficiency of cephalexin decreased and therefore, maximum removal occurred at 10 °C. Reduction of adsorption efficiency with temperature increase can be attributed to higher turbulence, which weakens the electrostatic attraction forces between the adsorbent and the antibiotic [37].

Thermodynamic studies of an adsorption process are necessary to evaluate whether the process is spontaneous or not. The Gibbs free energy change,  $\Delta G^\circ$ , as an indication of spontaneity of a chemical reaction, is an important factor for spontaneity. Both entropy and energy items must be calculated to determine  $\Delta G^\circ$  value of the

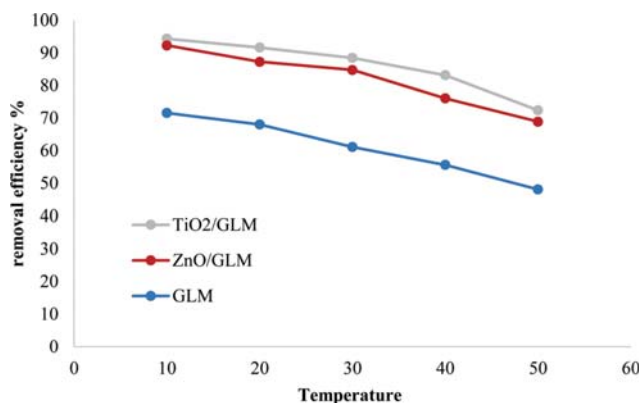


Fig. 12. Effect of temperature on cephalexin adsorption by GLM, ZnO/GLM and TiO<sub>2</sub>/GLM (pH=2, dosage=4 g/L, agitation speed=150 rpm, cephalexin concentration=25 mg/L, contact time=60 min).

adsorption process.

The van't Hoff equation was applied to calculate thermodynamic parameters, which is defined as:

$$K_d = \frac{q_e}{C_e} \times \rho \quad (1)$$

$$\Delta G^\circ = -RT \ln K_d \quad (2)$$

$$\ln K_d = \frac{\Delta S^\circ}{R} - \frac{\Delta H^\circ}{RT} \quad (3)$$

where,  $K_d$  is the thermodynamic equilibrium constant,  $q_e$  is the amount of cephalexin adsorbed (mg/g),  $C_e$  is cephalexin concentration (mg/L),  $\rho$  is the density of the solution ( $\rho=1,000$  g/L),  $\Delta G^\circ$  is the standard free energy change (J/mol),  $T$  is the absolute temperature (K) and  $R$  is the gas constant (8.314 J/mol·K) [38].

The standard entropy change ( $\Delta S^\circ$ ) and the standard enthalpy change of adsorption ( $\Delta H^\circ$ ) are calculated from the intercept and

Table 1. Thermodynamic data for adsorption of cephalexin by GLM, ZnO/GLM, and TiO<sub>2</sub>/GLM

Adsorbents	T (K)	$\Delta G^\circ$ (kJ/mol)	$\Delta S^\circ$ (J/mol.k)	$\Delta H^\circ$ (kJ/mol)
GLM	283	-15.16	-13.68	<b>-19.16</b>
	293	-15.29		
	303	-15.05		
	313	-14.95		
	323	-14.62		
ZnO/GLM	283	-18.83	-44.79	<b>-31.48</b>
	293	-18.14		
	303	-18.23		
	313	-17.37		
	323	-16.96		
TiO <sub>2</sub> /GLM	283	-19.62	-50.57	<b>-34.10</b>
	293	-19.28		
	303	-19.04		
	313	-18.52		
	323	-17.41		

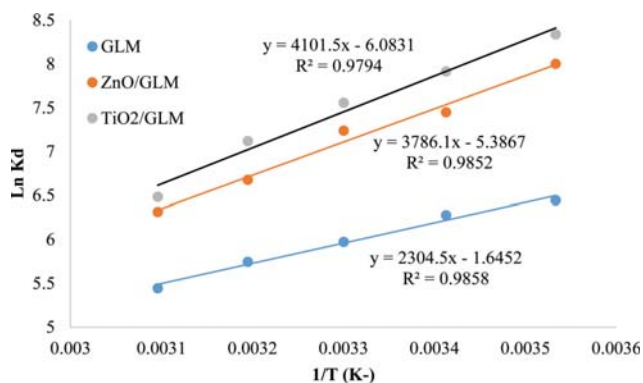


Fig. 13. van't Hoff plots for the adsorption of cephalaxin by GLM, ZnO/GLM, and TiO<sub>2</sub>/GLM.

Table 2. Non-linear forms of isotherm models of Langmuir, Freundlich, Temkin and Redlich-Peterson

Langmuir	$q_e = \frac{Q_m K_a C_e}{1 + K_a C_e}$
Freundlich	$q_e = K_f C_e^{1/n_F}$
Temkin	$q_e = \frac{RT}{B_T} \ln(K_T C_e)$
Redlich-Peterson	$q_e = \frac{A_{RP} C_e}{(1 + B_{RP} C_e^g)}$

Table 3. Parameters of isotherm models of Langmuir, Freundlich, Temkin and Redlich-Peterson

Isotherm model	Adsorbents		
	GLM	ZnO/GLM	TiO <sub>2</sub> /GLM
Langmuir			
Q <sub>m</sub> (mg/g)	7.82	17.09	49.26
K <sub>L</sub> (L/mg)	0.016	0.02	0.009
R <sup>2</sup>	0.96	0.983	0.996
Δq <sub>e</sub> (%)	12.14	11.26	5.38
Freundlich			
K <sub>F</sub> (mg/g)	0.53	1.32	1.04
n <sub>F</sub>	2.13	2.15	1.45
R <sup>2</sup>	0.987	0.975	0.985
Δq <sub>e</sub> (%)	5.35	10.06	13.5
Temkin			
K <sub>T</sub> (L/g)	0.18	0.22	0.14
B <sub>T</sub> (J/mol)	1.66	3.68	8.71
R <sup>2</sup>	0.966	0.977	0.978
Δq <sub>e</sub> (%)	9.61	13.59	23.34
Redlich-Peterson			
A <sub>RP</sub> (L/mg) <sup>-g</sup>	0.30	0.39	0.38
B <sub>RP</sub> (L/g)	0.23	0.035	0.00008
g	0.68	0.92	1.93
R <sup>2</sup>	0.981	0.978	0.999
Δq <sub>e</sub> (%)	6.58	10.41	5.11

slope of van't Hoff plot (ln K versus 1/T), respectively. The thermodynamic parameters related to the adsorption process are summarized in Table 1 and van't Hoff diagram in Fig. 12. The values of ΔG° were negative at all reaction temperatures studied, which indicates that the adsorption process of cephalaxin by GLM, ZnO/GLM and TiO<sub>2</sub>/GLM is spontaneous over the range of temperatures studied. Additionally, the results illustrated that enthalpy values (ΔH°) was negative for all the three adsorbents, which demonstrates that the adsorption process is exothermic. Furthermore, negative ΔS° values were obtained, which indicates a decrease in randomness at the solid-solution interface during the adsorption of the antibiotic onto the adsorbents [39].

9. Isotherm Studies

Adsorption isotherms describe the relationship between adsorbate and adsorbent in a system, determining the maximum adsorption capacity of an adsorbent and estimate the possible adsorp-

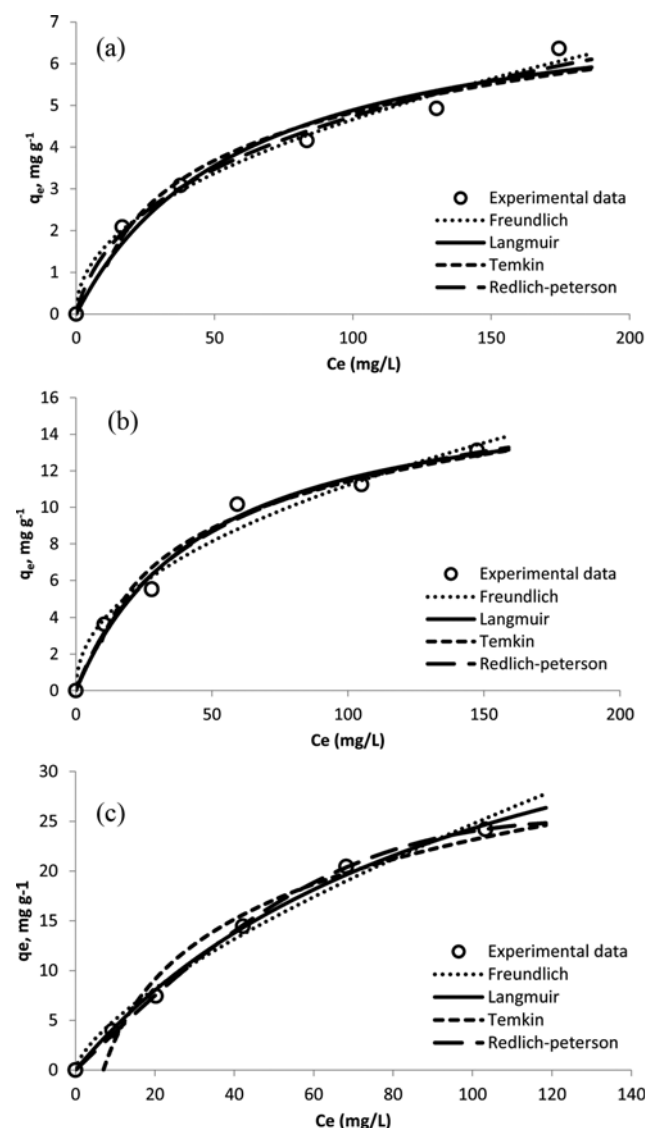


Fig. 14. Plots of Freundlich, Langmuir, Temkin and Redlich-Peterson models for cephalaxine adsorption onto the GLM (a), ZnO/GLM (b) and TiO<sub>2</sub>/GLM (c).

tion mechanism of a pollutant [40]. The equilibrium experimental data in the present study were then fitted to the Freundlich, Langmuir, Temkin and Redlich-Peterson models to evaluate removal behavior and estimate model parameters for cephalexin adsorption by GLM, ZnO/GLM, and TiO<sub>2</sub>/GLM. The nonlinear diagrams of these isotherms are shown in Fig. 14 and their models are given in Table 2. Origin 6.1 software was used to fit the experimental data to nonlinear forms of isotherms.

Langmuir model describes monolayer adsorption of an adsorbent on a homogeneous surface [41]. As shown in Table 3, the maximum adsorption capacities (Q<sub>m</sub>) were obtained to be 7.82, 17.09 and 49.26 mg/g for GLM, ZnO/GLM and TiO<sub>2</sub>/GLM, respectively. Based on the table, the value of Q<sub>m</sub> for TiO<sub>2</sub>/GLM is much more than those of two other adsorbents, indicating the important role of nanoparticle loading in the enhancement of adsorption efficiency of the pollutant. Freundlich isotherm is an empirical model which describes the adsorption of an adsorbate on an adsorbent on a heterogeneous surface. Heterogeneity factor, n<sub>F</sub>, can also be employed to describe the system's heterogeneity when n<sub>F</sub>=1, the adsorption is linear, n<sub>F</sub><1 implies chemical and n<sub>F</sub>>1 represents physical adsorption [42]. As shown in Table 3, the value of n<sub>F</sub> for GLM, ZnO/GLM and TiO<sub>2</sub>/GLM are 2.13, 2.15 and 1.45, respectively. The values of n<sub>F</sub> for all of these adsorbents are above 1, indicating the physical adsorption of cephalexin on the adsorbents.

Temkin isotherm assumes that the adsorption heat of all the molecules in layer diminishes linearly with coverage due to interactions between adsorbent-adsorbate. Temkin constant, B<sub>T</sub>, is related to the heat of adsorption. When 1<B<sub>T</sub>, the adsorption process is exothermic and vice versa [41,43]. According to Table 3, the amount of B<sub>T</sub> is above 1 for these three adsorbents (GLM=1.66, ZnO/GLM=3.68 and TiO<sub>2</sub>/GLM=8.71), representing their exothermic nature for the adsorption of cephalexin. These findings also agree with the results of thermodynamic studies.

The Redlich-Peterson is an empirical adsorption model which has three parameters. It can be applied to represent adsorption equilibrium over a wide range of concentration. It features some parameters from both the Langmuir and Freundlich isotherm, and consequently, it may be employed either in homogeneous or heterogeneous conditions. In Redlich-Peterson equation, g is an exponent between 0 and 1. When g=1, the Redlich-Peterson model is closer to the Langmuir isotherm equation, and when g=0, it becomes the Freundlich equation [40]. In the present study, the value of g for all three adsorbents was unity, indicating the Langmuir isotherm model gives a better fit to the obtained experimental data.

## CONCLUSION

The present study revealed that green local montmorillonite (GLM) coated with ZnO and TiO<sub>2</sub> in the presence of H<sub>2</sub>O<sub>2</sub> could be cheap and effective adsorbents for the removal of cephalexin from aqueous solutions. Loading ZnO and TiO<sub>2</sub> nanoparticles onto GLM changed the pore size distribution, produced more functional groups, and improved the antibiotic adsorption capacity. TiO<sub>2</sub>/GLM showed a better adsorption for cephalexin as compared to ZnO/GLM.

SEM analysis showed that the nanoparticle coated onto GLM in the presence of H<sub>2</sub>O<sub>2</sub> provided a rough surface with a highly porous structure and greater surface area suitable for loading the antibiotic. XRD patterns showed the appearance of new peaks onto GLM after coating with TiO<sub>2</sub> and ZnO. The thermodynamics parameters revealed that the adsorption process was spontaneous and exothermic.

## ACKNOWLEDGEMENTS

The authors thank Ardabil University of medical sciences because of their financial support.

## REFERENCES

1. Q. Wu, Z. Li, H. Hong, K. Yin and L. Tie, *Appl. Clay Sci.*, **50**(2), 204 (2010).
2. E. Azizl, M. Fazlzadeh, M. Ghayebzadeh, L. Hemati, M. Beikmohammadi, H. R. Ghaffari, H. R. Zakeri and K. Sharafi, *Environ. Protection Eng.*, **43**(1), 183 (2017).
3. A. J. Watkinson, E. J. Murby and S. D. Costanzo, *Water Res.*, **41**(18), 4164 (2007).
4. H. R. Gaskins, C. T. Collier and D. B. Anderson, *Animal Biotechnol.*, **13**(1), 29 (2002).
5. T. A. Ternes, A. Joss and H. Siegrist, *Environ. Sci. Technol.*, **38**(20), 392a (2004).
6. S. Thiele-Bruhn, *J. Plant Nutrition Soil Sci.*, **166**(2), 145 (2003).
7. M.-S. Miao, Q. Liu, L. Shu, Z. Wang, Y.-Z. Liu and Q. Kong, *Process Safety Environ. Protection*, **104**, Part B, 481 (2016).
8. Q. Kong, Y.-n. Wang, L. Shu and M.-s. Miao, *Desalination Water Treatment*, **57**(17), 7933 (2016).
9. M. J. Ahmed and S. K. Theydan, *Chem. Eng. J.*, **211**, 200 (2012).
10. M. Fazlzadeh, K. Rahmani, A. Zarei, H. Abdoallahzadeh, F. Nasiri and R. Khosravi, *Adv. Powder Technol.*, **28**(1), 122 (2017).
11. R. Khosravi, M. Fazlzadehdavil, B. Barikbin and A. A. Taghizadeh, *Appl. Surface Sci.*, **292**, 670 (2014).
12. M. Pirsahab, A. Dargahi, S. Hazrati and M. Fazlzadehdavil, *Desalination Water Treatment*, **52**(22-24), 4350 (2014).
13. G. K. Sarma, S. S. Gupta and K. G. Bhattacharyya, *J. Environ. Manage.*, **171**, 1 (2016).
14. M. Fazlzadeh, A. Ahmadfazeli, A. Entezari, A. Shaegi and R. Khosravi, *Koomesh*, **18**(3), 388 (2016).
15. J. Méndez-Díaz, G. Prados-Joya, J. Rivera-Utrilla, R. Leyva-Ramos, M. Sánchez-Polo, M. Ferro-García and N. Medellín-Castillo, *J. Colloid Interface Sci.*, **345**(2), 481 (2010).
16. H. Abdoallahzadeh, B. Alizadeh, R. Khosravi and M. Fazlzadeh, *J. Mazandaran University Medical Sciences*, **26**(139), 111 (2016).
17. S. Parastar, S. Nasseri, S. H. Borji, M. Fazlzadeh, A. H. Mahvi, A. H. Javadi and M. Gholami, *Desalination Water Treatment*, **51**(37-39), 7137 (2013).
18. M. Fazlzadeh, R. Khosravi and A. Zarei, *Ecological Engineering*, **103**, 180 (2017).
19. M. Leili, M. Fazlzadeh and A. Bhatnagar, *Environ. Technol.*, United Kingdom, **1** (2017).
20. D. K. Tiwari, J. Behari and P. Sen, *World Appl. Sci. J.*, **3**(3), 417 (2008).

21. M. Fazlzadeh, H. Abdoallahzadeh, R. Khosravi and B. Alizadeh, *J. Mazandaran University Medical Sciences*, **26**(143), 174 (2016).
22. N. Lian, X. Chang, H. Zheng, S. Wang, Y. Cui and Y. Zhai, *Microchim. Acta*, **151**(1), 81 (2005).
23. Q. Shi, J. Zhang, C. Zhang, W. Nie, B. Zhang and H. Zhang, *J. Colloid Interface Sci.*, **343**(1), 188 (2010).
24. C. Mena-Duran, M. S. Kou, T. Lopez, J. Azamar-Barrios, D. Aguilar, M. Dominguez, J. A. Odriozola and P. Quintana, *Appl. Surface Sci.*, **253**(13), 5762 (2007).
25. M. Golmohammadi, J. Towfighi, M. Hosseinpour and S. J. Ahmadi, *J. Supercritical Fluids*, **107**, 699 (2016).
26. Y. Xue, B. Gao, Y. Yao, M. Inyang, M. Zhang, A. R. Zimmerman and K. S. Ro, *Chem. Eng. J.*, **200**, 673 (2012).
27. M. M. Silva, M. M. Oliveira, M. C. Avelino, M. G. Fonseca, R. K. Almeida and E. C. Silva Filho, *Chem. Eng. J.*, **203**, 259 (2012).
28. X. Ren, Z. Zhang, H. Luo, B. Hu, Z. Dang, C. Yang and L. Li, *Appl. Clay Sci.*, **97-98**, 17 (2014).
29. M. Ghaedi, A. G. Nasab, S. Khodadoust, R. Sahraei and A. Daneshfar, *J. Ind. Eng. Chem.*, **21**, 986 (2015).
30. A. B. Albadarin, C. Mangwandi, A. a. H. Al-Muhtaseb, G. M. Walker, S. J. Allen and M. N. M. Ahmad, *Chem. Eng. J.*, **179**, 193 (2012).
31. G. Nazari, H. Abolghasemi and M. Esmaili, *J. Taiwan Inst. Chem. Engineers*, **58**, 357 (2016).
32. M. S. Legnoverde, S. Simonetti and E. I. Basaldella, *Appl. Surface Sci.*, **300**, 37 (2014).
33. H. R. Pouretedal and N. Sadegh, *J. Water Process Eng.*, **1**, 64 (2014).
34. M. Ghaedi, M. Ghayedi, S. N. Kokhdan, R. Sahraei and A. Daneshfar, *J. Ind. Eng. Chem.*, **19**(4), 1209-17 (2013).
35. Z. Noorimotlagh, R. D. C. Soltani, G. S. Khorramabadi, H. Godini and M. Almasian, *Desalination Water Treatment*, **57**(4), 1684 (2016).
36. I. Turku, T. Sainio and E. Paatero, *Environ. Chem. Lett.*, **5**(4), 225 (2007).
37. G. Moussavi, A. Alahabadi, K. Yaghmaeian and M. Eskandari, *Chem. Eng. J.*, **217**, 119 (2013).
38. S. K. Milonjić, *J. Serbian Chem. Soc.*, **72**(12), 1363 (2007).
39. Ş. S. Bayazit and Ö. Kerkez, *Chem. Eng. Res. Design*, **92**(11), 2725 (2014).
40. O. Pezoti, A. L. Cazetta, I. P. Souza, K. C. Bedin, A. C. Martins, T. L. Silva and V. C. Almeida, *J. Ind. Eng. Chem.*, **20**(6), 4401 (2014).
41. A. C. Martins, O. Pezoti, A. L. Cazetta, K. C. Bedin, D. A. Yamazaki, G. F. Bandoch, T. Asefa, J. V. Visentainer and V. C. Almeida, *Chem. Eng. J.*, **260**, 291 (2015).
42. A. L. Cazetta, A. M. Vargas, E. M. Nogami, M. H. Kunita, M. R. Guilherme, A. C. Martins, T. L. Silva, J. C. Moraes and V. C. Almeida, *Chem. Eng. J.*, **174**(1), 117 (2011).
43. G. Moussavi and R. Khosravi, *J. Hazard. Mater.*, **183**(1), 724 (2010).